the several mechanisms to control cell-to-cell communications between pancreatic β-cells, the one mediated by gap junctions is believed to be essential for the recruitment and synchronization of insulin-secreting cells. Previous studies showed that the proper insulin secretion from pancreatic islets depends on a communication network coordinating the activities of individual insulin-producing cells. The single β-cells unconnected with connexin channels show poor expression of the insulin gene and release low amounts of the hormone after stimulation, whereas both insulin biosynthesis and release are rapidly improved due to the restoration of β-cell contacts [1, 2]. It is known that HA-treatment enhances the function of GJIC in normal human dermal fibroblasts [3] and the expression of Connexin43 in rat calvarial osteoblast [4]. In this study, we used HIT-T15 cells, the clonal pancreatic β-cell line, to observe the relative effect of HA on insulin secretion and gap-junctions between β-cells. The results obtained indicate that HA increases insulin secretion of HIT-T15 cells by the enhancement of GJIC.

2.   MATERIALS AND METHODS

2.1   Preparation of media and culture dishes

The high-molecular-weight (HMW) HA polysaccharide was dissolved in distilled water at a concentration of 4 mg/ml. Each 35-mm culture dish was coated at a final concentration of 0.01 to 2.0 mg/ml. The HA-coated dishes were dried further under sterile air flow at room temperature for 12 h before use. In order to investigate the effect of HA-addition on the functions of HIT-T15 cells, many media were prepared with various concentrations of HA.

2.2   Cell culture

The hamster pancreatic β-cell line, HIT-T15, were cultured in RPMI 1640 medium containing 10% fetal bovine serum (FBS), 2 mM L-glutamine, 25 mM HEPES, 100 IU/ml penicillin-G and 100 µg/ml streptomycin. HIT-T15 cells in RPMI 1640 medium were maintained in a humidified 5% CO_2 incubator at 37°C. The subcultured cells were seeded at a density of $1.0 \sim 5.0 \times 10^5$ cells/ml in multiwell plates or culture dishes. When they reached more than 80% confluence, the cells were used for various studies. Throughout the cell growth period the culture media were exchanged every 2-3 days.

2.3   Measurement of cell viability

HIT-T15 cells (1×10^5) were incubated into the various concentrations of HA-coated 24 wells plate, or after the cells were seeded onto 24 well plates and pre-incubated in a 10%FBS/RPMI 1640 medium overnight, the medium was exchanged for 10%FBS/HA/RPMI 1640 medium prepared. After 72 h of HA-treatment, the cell viability was determined by alamarBlue™ assay, according to the manufacturer instructions. Control cells received fresh medium without HA.

2.4   Measurement of insulin release

HIT-T15 cells were treated as described above. After washing with KRB buffer, the cells were incubated with KRB buffer for 60 min. The amount of insulin release in the spent medium was determined by ELISA insulin kit, according to the manufacturer instructions.

2.5   Scrape-loading and dye transfer (SLDT) assay

HIT-T15 cells (5×10^5) were treated as described above. The cells were washed three times with PBS (+) before the addition of the fluorescent dye. The cells were scraped using a surgical blade and loaded with 0.1% Lucifer Yellow solution for 5 min at 37°C. The dye solution was discarded, washed three times with PBS (+) solution to remove detached cells and background fluorescence. The distance of dye transfer was measured at room temperature under the fluorescence microscope equipped with a type UFX-DXII and Super High Pressure Mercury Lamp Power Supply (NIKON, Japan).

3.   RESULTS AND DISCUSSION

In order to evaluate the effect of HA on cell viability, HIT-T15 cells were treated with HA-coated or -added for 72 h. At the same incubated time, the cell viability of HIT-T15 cells grown on high concentration HA-coated dishes ($\geq$ 2.0 mg/dish) was significantly less than low concentration HA-coated and control (Fig. 1). However, there was no difference in cell viability between the HA-added and control (data not shown). Previous studies have shown that HMW (310 kDa and 800 kDa) HA-coating resulted in low adhesiveness to the cells. Because the HMW HA-coated surface provides a stable anionic surface that prevents cells attachment at the early time. In this study, after 12 h, the cells in low

Yuping Li et al.

concentration HA (1680 kDa)-coated dishes (0.01, 0.5, 1.0 mg/dish) already had attached and confluent but not in high concentration HA-coated dishes (2.0 mg/dish). These results indicated that the changes of cell viability by HA-treatment may depend on the cell attachment activity.
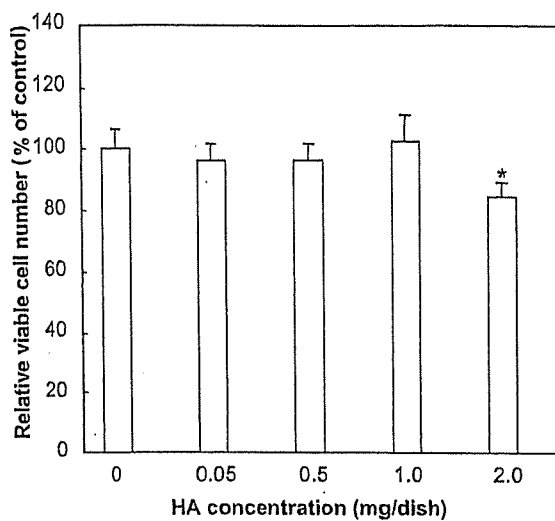

Figure 1. Viability of HIT-T15 cell after 72 h of HA-treatment. The viable cell numbers of HIT-T15 cell were determined by alamarBlue^{TM} assay as described in Section 2. Each value denotes the mean ± S.D. *$P \leq 0.05$ compared to untreated control.

HIT-T15 cells, retain glucose-stimulated insulin secretion, showed a increase in insulin secretion as a function of stimulation. Thus, their insulin output was 13.25 ± 0.96 and 19.63 ± 0.98 pg/µg protein in the base and glucose-stimulation (11.1 mM), respectively (n = 9 dishes from three independent experiments) (data not shown). When these cells were exposed to low concentration of HA-coating (0.25, 0.5. 1.0 mg/dish), their insulin secretion was significantly increased in the absence or presence of glucose-stimulation. By contrast, high concentration of HA-coating (2.0 mg/dish) failed to increase its insulin secretion (Fig. 2).

On the other hand, when HIT-T15 cells were treated with HA-addition for 72 h, the increasing effect was not exhibited. The insulin secretion was without difference between control and HA-addition (data not shown). Previous studies have indicated that HA-treatment enhances the function of GJIC in normal human dermal fibroblasts [3] and the expression of Connexin43 in rat calvarial osteoblast [4]. The increasing evidence suggests that gap junction proteins and/or GJIC participate in the multifactorial control of insulin secretion. Thus, the increase in insulin secretion by HA-coating might have relation to gap junctions.
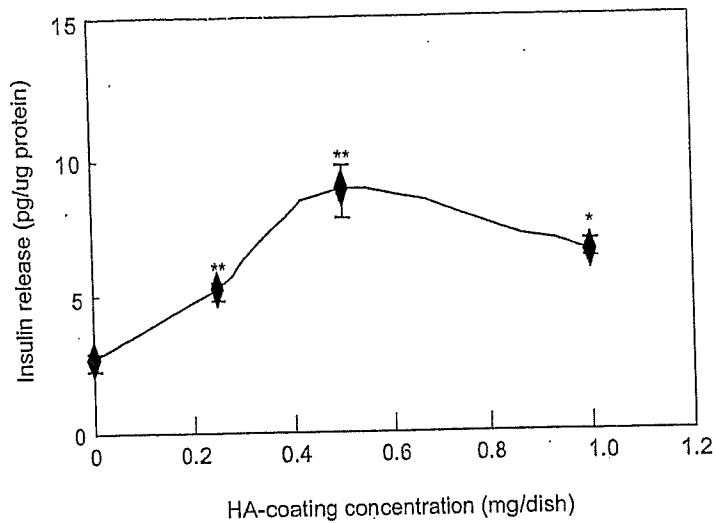
Figure 2. Concentration-dependent effects of HA-coating on insulin secretion from HIT-T15 cells. Treated with HA for 72 h, HIT-T15 cells were incubated with KRB buffer for 60 min. The released insulin in the spent medium was determined by ELISA insulin kit. Each value denotes the mean ± S.D. of three separate experiments. $*P \leq 0.05$, $**P \leq 0.01$ compared to control.

To test whether the HA-coating affects the gap junctions in pancreatic β-cells, we assessed the function of GJIC using Lucifer Yellow by SLDT assay. A scrape line was made on the cell grown to confluence, and the fluorescent dye penetrated the adjacent cells. The distance of dye transfer was determined.
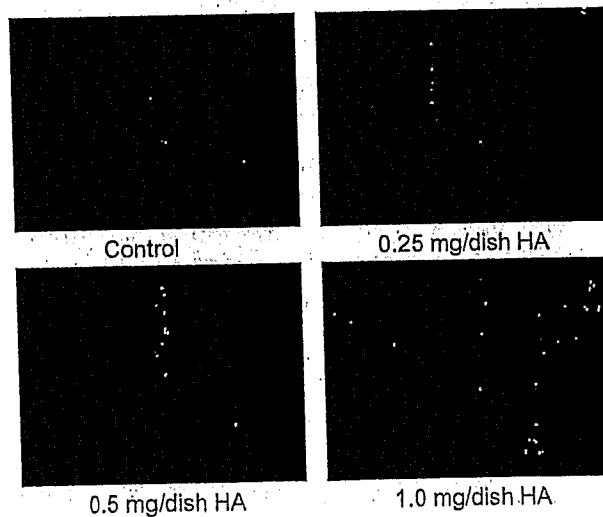

Figure 3. Time-course effects of various concentrations of HA-coating on the dye transfer ratio of HIT-T15 cells.

Fig. 3 shows the patterns of dye transfer in HIT-T15 cells treated with HA. The dye transfer extent of the cells grown on the HA-coated dishes

was more than that of the control, which indicated that GJIC function was activated by the HA-coating. The effect of HA is influenced by the concentration of FBS and the nutrients in medium, because the serum contains many components such as hormone, growth factor (FGF, etc.), cell adhesion molecule (N-CAM and cadherins), and transportation protein [4]. As a result, the HIT-T15 cells can use these nutrients and the nutrient-enriched substrata, e.g., natural extracellular matrixes with HA bound, to change the cell aggregations. Therefore, HA might play an important role in the increase of GJIC.

With the evidence above, it is known that the gap junction channels play a role in the regulation of β-cell secretion [5, 6]. It has been shown that the increase in connexin, e.g., gap junction proteins Cx43, affects the electrical coupling, synchronization of $[Ca^{2+}]_i$ oscillations, and insulin secretion, and the insulin secretion is evoked by a variety of metabolizable and nonmetabolizable secretagogues that activate different intracellular pathways [7-10]. In this study, we have found that the functional gap junction is promoted by low concentration HA-coating in spite of the inhibitory effects on the cell viability in high concentration HA-coating dishes. However, further intensive investigation should be promoted on the detailed action mechanism of HMW-HA responsible for the insulin-secreting activity.

4. CONCLUSIONS

The function of GJIC is considered to be a useful marker for evaluating tissue-engineered products. The data obtained in this study shows that gap junctions contribute to regulating some still-unknown mechanism to couple the stimulus-secretion of HIT-T15 cells under the condition of low concentration HA-coating. These results give useful information on how to design biomaterials of polysaccharides such as HA, when the GJIC is an important function for evaluating biocompatibility of biomaterials.

5. REFERENCES

1. Meda P., Bosco D., Chanson M., Giordano E., Vallar L., Wollheim C. and Orci L. (1990) Rapid and reversible secretion changes during uncoupling of rat insulin-producing cells. *J Clin Invest* 86:759-768

2. Vozzi C., Ullrich S., Charollais A., Philippe J., Qeci L. and Medz P. (1995) Adequate connexin-mediated coupling is required for proper insulin production. *J Cell Biol* 131: 1561-1572

3. Park JU. and Tsuchiya T. (2002) Increase in gap-junctional intercellular communications (GJIC) of normal human dermal fibroblasts (NHDF) on surfaces coated with high-molecular-weight hyaluronic acid (HMW HA). *Inc J Biomed Mater Res* 60: 541-547

4. Nagahata M., Tsuchiya T., Ishiguro T., Matsuda N., Nakatsuchi Y., Teramoto A., Hachimori A. and Abe K. (2004) Anovel function of N-cadherin and Connexin 43: marked enhancement of alkaline phosphatase activity in rat calvarial osteoblast exposed to sulfated hyaluronan. *Biochem Biphys Res Commun* 315: 603-611

5. Meda P. (1996) The role of gap junction membrane channels in secretion and hormonal action. *J Bioenery Biomembr* 28: 369-377

6. Charollais A., Gjinovci A., Huarte J., Bauquis J., Nadal A., Martin F., Andreu E., Sanchez-Andres JV., Calabrese A., Bosco D., Soria B.,m B., Herrera PL. and Meda P. (2000) Junctional communication of pancreatic beta cells contribetes to control of insulin secretion and glucose tolerance. *J Clin Invest* 106: 235-243

7. Cakabrese A., Zhang M., Serre-Beinier V., Caton D., Mas C., Satin SL. and Meda P. (2003) Connexin 36 controls synchronization of Ca^{2+} oscillations and insulin secretion in MIN6 cells. *Diabetes* 52: 417-424

8. Meda P., Chanson M. and Pepper M. (1991) *In vivo* modulation of connexin-43 gene expression an djunctional coupling of pancreaticc β-cells. *Exp Cell Res* 192: 469-480

9. Meda P., Pepper MS. and Traub O. (1993) Differential expression of gap junction connexins in endocrine and exocrine glands. *Endocrinology* 133: 2371-2378

10. Charollais A., Serre V., Mock C., Cogne F., Bosco D. and Meda P. (1999) Loss of α_1 connexin does not alter the prenatal differentiation of pancreatic β-cells and leads to the identification of another islet cell connexin. *Dev Genetics* 24: 13-26

SAFETY EVALUATION OF TISSUE ENGINEERED MEDICAL DEVICES USING NORMAL HUMAN MESENCHYMAL STEM CELLS

Rumi Sawada, Tomomi Ito, Yoshie Matsuda, and Toshie Tsuchiya
Division of Medical Devices, National Institute of Health Sciences

Abstract: For safety evaluation of tissue engineered medical devices using normal human mesenchymal stem cells (hMSC), in this study, some genes expressions in hMSC were compared with those in two kinds of the tumor cells (HeLa and HepG2). Effects of the passage number of hMSC on the gene expressions were also investigated using quantitative real-time RT-PCR. The proliferation speed of hMSC was lowered with the cell passage number. The mRNA expressions of c-myc oncogene and nucleostemin in the tumor cells (HeLa and HepG2) were significantly higher than in the stem cells (hMSC). And the mRNA expressions of them in hMSC decreased with the passage number. Wnt-8B mRNA was expressed in the tumor cells (HeLa and HepG2), but not in the stem cells (hMSC) in any passage number. Although these results suggest change in these expression levels are not directly related to the tumorigenesis of hMSC, it is discussed that mRNA expression levels of c-myc oncogene, nucleostemin, and Wnt-8B can be used as an index of hMSC tumorigenesis.

Key words: hMSC, tumorigenesis, c-myc, nucleostemin, Wnt-8

1.   INTRODUCTION

Several recent studies demonstrate the potential of tissue engineering for regenerative therapy using somatic stem cells. Human mesenchymal stem cells (hMSC) derived from bone marrow aspirates have the potentiality to differentiate into osteocytes, chondrocytes, myocytes, stromal cells, tenocytes, adipocytes, and so on. Therefore, the autologous cell or tissue transplantation using hMSC was noticed as the medical treatment under the various kinds of clinical conditions. On the

326

Rumi Sawada et al.

other hand, owing to the similarity to the tumor cells, the stem cells also possess the ability of cell proliferation. Consequently, it is required to evaluate the safety of hMSC when that is used for tissue engineered medical devices. In this study, hMSC was compared with two kinds of the the tumor cells, HeLa (human cervix cancer) and HepG2 (human hepatoma), by investigating the differences in some genes expressions of each cells. Effects of the passage number of hMSC on the gene expressions were also investigated using quantitative real-time RT-PCR.

2. MATERIALS AND METHODS

Cell culture. Human mesenchymal stem cells (hMSC) purchased from the Cambrex Bio Science Walkersville, Inc. (MD, USA) was cultured in Mesenchymal Stem Cell Basal Medium (MSCBM; Cambrex Bio Science Walkersville, Inc.) supplemented with Mesenchymal Cell Growth Supplement (MCGS; Cambrex Bio Science Walkersville, Inc.), L-Glutamine and Pen/Strep at 37°C under a 5% CO_2 atmosphere. The cells was seeded at a density of 6,000 cells / cm^2 and subcultured when they are just sub-confluent (approximately 90% confluent) up to 10th passage.

Quantitative RT-PCR. For quantitative RT-PCR, total RNA was extracted from hMSC of 1st, 3rd, 5th and 10th passage cultures with ISOGEN (NIPPON GENE CO., LTD.). RNA was then reverse-transcribed into cDNA using First Strand cDNA Synthesis Kit for RT-PCR (AMV) (Roche Diagnostics; Tokyo, Japan). Primers and annealing temperatures for the c-myc oncogene, nucleostemin, and Wnt-8B are summarized in Table 1. Amplifications of them were carried out for 10s at 95°C, for 15s at each annealing temperature, and for 12s at 72°C for 40 cycles. PCR was performed in Light Cycler Fast Start DNA Master SYBR Green I (Roche Diagnostics) in Roche Light Cycler (software version 4.0).

Table 1. Primers and annealing temperatures used for Real time RT-PCR

Gene name	GenBank™ accession number	Primer orientation	Nucleotide sequence	Starting sequence position	Size for the PCR amplicon(bp)	Annealing Temp ("c)
c-myc	V00568	Forward Reverse	5'- GCG AAC ACA CAA CGT C -3' 5'- CAA GTT CAT AGG TGA TTG CT -3'	1626 1940	315	50
nucleostemin	X91940	Forward Reverse	5'- CCA TTC GGG TTG GAG TAA -3' 5'- CTG TCG AGC ATC AGC C -3'	782 1065	284	50
Wnt-8B	NM_014366	Forward Reverse	5'- AGT GAC AAT GTG GGC T -3' 5'- CGT GGT ACT TCT CCT TCA G -3'	331 574	244	60

3.　RESULTS

In this study, for safety evaluation of tissue engineered medical devices using normal human mesenchymal stem cells (hMSC), some genes expressions in hMSC were compared with those in two kinds of the tumor cells (HeLa and HepG2). At first, effect of the passage number on hMSC proliferlation was investigated. The proliferation speed of hMSC was lowered with the cell passage number (Fig. 1).
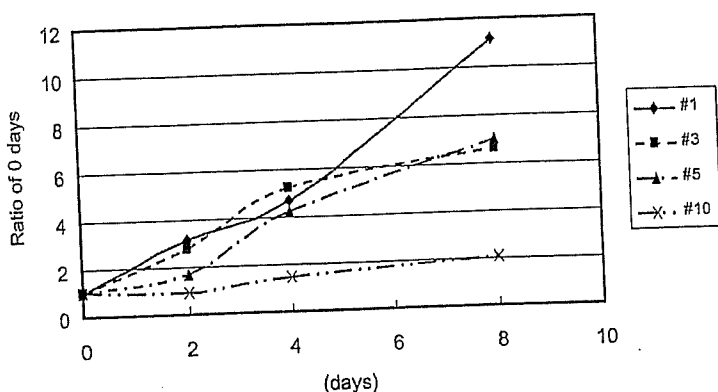

Fig. 1. Effect of the passage number on the cell growth curves of hMSC.

The mRNA expressions of c-myc oncogene in the tumor cells (HeLa and HepG2) were significantly higher than in the stem cells (hMSC) (Fig. 2). The mRNA expressions of c-myc oncogene in hMSC in the 3rd and 5th passages were higher than in the 1st and 10th passages (Fig. 3). Similarly to c-myc, the mRNA expressions of nucleostemin in the tumor cells (HeLa and HepG2) were significantly higher than in the stem cells (hMSC) (Fig. 4). The mRNA expressions of nucleostemin in hMSC decreased with the passage number (Fig. 5). Wnt-8B mRNA was expressed in the tumor cells (HeLa and HepG2), but not in the stem cells (hMSC) in any passage number (Fig. 6).
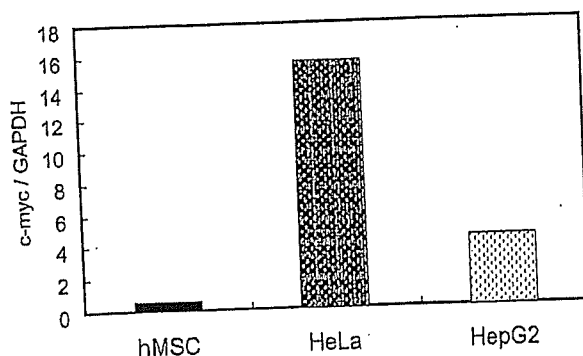

Fig. 2. The mRNA expression c-myc oncogene in hMSC, HeLa, and HepG2.
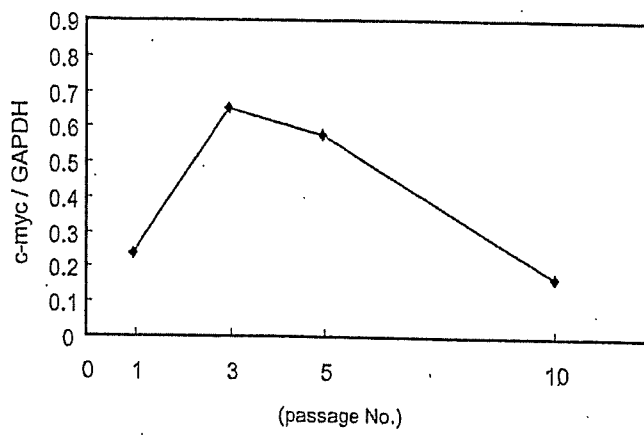
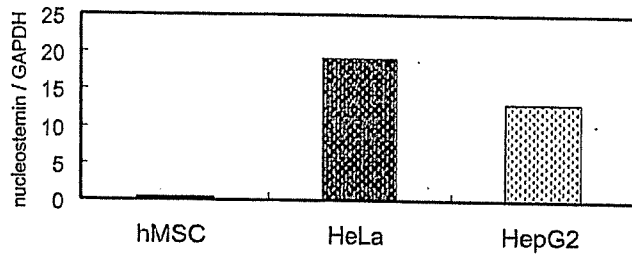Fig. 3. Effect of the passage number on the mRNA expression c-myc oncogene in hMSC.

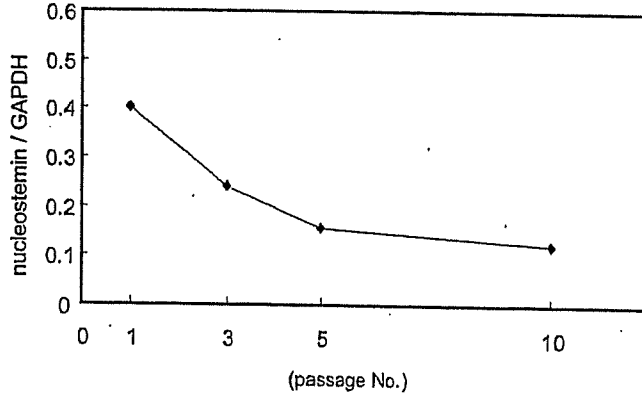Fig. 4. The mRNA expression nucleostemin in hMSC, HeLa, and HepG2.

Fig. 5. Effect og the passage number on the mRNA expression of nucleostemin in hMSC.
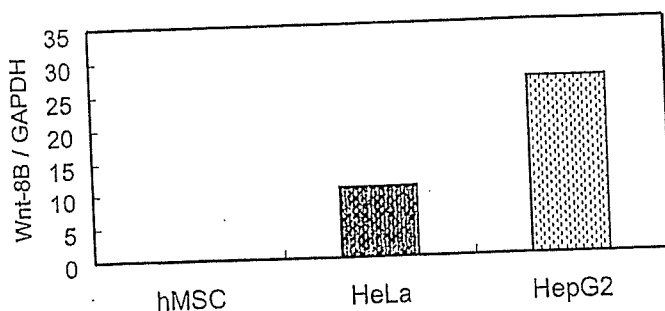
Fig. 6. The mRNA expression Wnt-8B in hMSC, HeLa, and HepG2.

4. DISCUSSION

In this study, effects of the passage number on the gene expression in hMSC were investigated. At first, c-myc oncogene and Wnt-8B concerned with cell proliferation and tumorigenesis were noticed by gene chip analysis (data not shown). Therefore, c-myc oncogene and Wnt-8B mRNA expressions in four kinds of passage numbers (#1, #3, #5, and #10) of hMSC were measured by quantitative real time RT-PCR. Furthermore, nucleostemin that concerned with proliferation of both stem cells and tumor cells (1) was also investigated. The proliferation speed of hMSC was lowered with the cell passage number (Fig. 1).

The mRNA expressions of c-myc oncogene, Wnt-8B, and nucleostemin in 1st, 3rd, 5th, and 10th passage of hMSC were investigated using quantitative real time RT-PCR. The mRNA levels of c-myc oncogene were decreased with the passage number from 3rd to 10th (Fig. 3). The mRNA expression of nucleostemin was decreased with the passage number (Fig. 5). In all three genes, their mRNA expressions of the stem cells (hMSC) were significantly lower than two kinds of tumor cells (HeLa and HepG2) (Fig. 2, 4, and 6). In hMSC, Wnt-8B was not expressed in any passage numbers. Although these results suggest that change in these expression levels are not directly related to the tumorigenesis of hMSC, it is discussed that mRNA expression levels of c-myc oncogene, nucleostemin, and Wnt-8B can be used as an index of hMSC tumorigenesis.

5. REFERENCES

1) Tsai R.Y.L. and McKay R.D.G., A nucleolar mechanism controlling cell proliferation in stem cells and tumor cells, *GENES & DEVELOPMENT* 16, 2991-3003 (2002).

EFFECT OF BIODEGRADABLE POLYMER POLY (L-LACTIC ACID) ON THE CELLULAR FUNCTION OF HUMAN ASTROCYTES

Naohito Nakamura and Toshie Tsuchiya
Departmetn of Medicdal Devices, National Institute of Health Science; Kamiyoga 1-18-1 Setagaya-ku, Tokyo, Japan

Abstract: The objective of this study is to assay the efficiency and safety of poly (L-lactic acid) (PLLA) on human neural tissues. We used normal human astrocytes (NHA) to clarify effects of PLLA on their proliferation and differentiation. We cultured NHA with PLLA for one week, and determined NHA cell number and neural cell specific marker genes to assay their proliferation and development, respectively.

Cell proliferation was determined by tetrazolium salt (MTT) assay. The cell number of astrocytes cultured with 50 µg/ml PLLA was 70% of control. It has been suggested that a part of astrocytes had neural precursor cell activity that give rise to neuron, oligodendrocyte and astrocyte. We compared gene expression of neural cell specific markers. Expression of Nestin, a specific gene for neural precursor cell was decreased in a dose-dependent manner, while expression of specific genes for neuron markers and astrocyte markers were not different from that of control.

PLLA suppressed astocyte proliferation in dose dependent manner. A neural precursor cell marker decreased when astrocytes were cultured with PLLA. These findings suggest that PLLA reduces proliferation and developmental potential of astrocytes.

Key words: Astrocyte, PLLA, proliferation, development

1.   INTRODUCTION

Brain and neural clinical hospitality have been rapidly advancing, including implantation techniques. Otherwise discreditable accidents sometimes happened. It is necessary to study efficiency and safety of techniques and materials for brain and neural cell proliferation and development. Precise mechanisms by which neurogenesis and gliogenesis are regulated in the central nervous system (CNS) remain to be elucidated. Telencephalic neuroepithelial cells contain neural precursors that give rise to the neuronal lineage and the glial lineage, which includes astrocytes and oliogodendrocytes (1, 2). The fate of neural precursors in the developing brain is believed to be determined by intrinsic cellular programs and by external cues, including implantation of biomaterials and cytokines (3). Doetsch et al. demonstrated that subventricular zone (SVZ) astrocytes act as neural stem cells in both the normal and regenerating brain (4). Neural stem cells, endogenously present in spinal cord *in vivo*, proliferate in response to injury, yet the vast majority of newly generate cells are glial fibrillary acidic protein (GFAP)-positive astrocytes (5). In addition, adult hippocampus-derived neural stem cells, when implanted into adult brain in such a region as cerebellum or striatum, have been reported to differentiate predominantly into glial cells (2, 6, 7).

Biodegradable polymers have been attractive candidates for scaffolding materials because they degrade and the new tissues are formed, although adverse events such as foreign-body reaction, inflammation and tumor formation were reported in clinical human and animal study. These scaffolds have shown great promise in the research of engineering a variety of tissues. Biodegradable polymer poly (L-lactic acid) (PLLA) is frequently implanted in cranial surgery etc. However, to engineer clinically useful tissues and organs is still a challenge. The understanding of the principles of scaffolding is far from satisfactory, still more its effect and safety on neural tissues are not known. We previously reported PLLA suppressed proliferation and differentiation of fetal rat midbrain neural precursor cells (8). In this report, we investigated the effect of PLLA on normal human astrocytes (NHA).

2.   MATERIALS AND METHODS

Astrocyte cell culture

We used normal human astrocyte (Cambrex Bio Science, Walkersville, MD). NHA were seeded into 12-well plates for quantitative RT-PCR at a density of 2 x 10^4/well, or 24-well plates for MTT assay at a density of 1 x 10^4/well in ABM medium(Cambrex Bio

Science) supplemented with 5% FCS, rhEGF and IGF, and cultured in a humidified atmosphere of 5% CO_2 in 95% air at 37°C.

PLLA preparation

Stock solutions of PLLA were made in dimethyl sulfoxide (DMSO) and final concentration of DMSO was 0.1%; this concentration did not affect proliferation and development of NHA. Control cultures were incubated with 0.1% DMSO. Stock solutions of lactic acid and tin chloride were made directly in ABM medium.

MTT assay

After cell culturing for 1 week with PLLA, the viability of NHA cells was determined by MTT assay. The TetraColor ONE (Seikagaku Kogyo, Tokyo, Japan) was used to measure changes of cell numbers. This assay is a nonradioactive alternative to tritium-thymidine incorporation. The system measures the conversion of tetrazolium salt compound into a soluble formazan product by the mitochondria of living cells. NHA in 24-well plates were cultured as described above. One week after NHA cultured with vehicle or PLLA, the media were replaced with 300 µl of fresh medium containing 6 µl TetraColor ONE reagent. After 2h, samples were measured in a micro plate reader.

Expression of neural cell marker genes

Total RNA was prepared from NHA using a modified acid guanidium thiocyanate-phenol-chloroform method. The total RNA treated with RNase-free DNase (Boehringer Mannheim, Mannheim, Germany) were subjected to reverse transcription using oligo d(T) primer (Toyobo, Tokyo, Japan) and superscript II reverse transcriptase (Gibco BRL, Gaithersburg, MD) at 42°C for 30 min followed by RNase H treatment. Aliquots of the cDNA (1/20) were used as templates for PCR analysis using Lightcycler system (Roche, Mannheim, Germany). PCR amplification was performed in a total volume of 20 µl mixture including 1 µl of RT reaction, 2 µl Light Cycler-Fast Start Reaction Mix SYBR Green 1(Roche, Mannheim, Germany), 0.5 µM/liter of each primer, and 3 mmol/liter $MgCl_2$. The PCR program consisted of 40 cycles of 8 sec at 94°C, 5 sec at 65°C, 10 sec at 72°C. Primer sequences for amplification are 5'- CTAAGGAGGAGATTGGACAGG-3' and 5'-AGTGGTGGCAGTGATTT CAGT-3' for Nurr-1 amplification, 5'-TCCGCTGCTCGCCGCTCCTAC-3' and 5'-TCATCTCTGCCCGCTCACTGG -3' for GFAP amplification, 5'-TCGCCCTGCCCACTTGACTTC-3' and 5'-TTCCACACCTCCACGCTC TGA-3' for Id-3 amplification, 5'-GAGATCAGAGCCCAGGATGCT-3' and 5'-CTGAGGGGTGGTGCCAAGGAG -3' for Nestin amplification, 5'-ACCACAGTCCATGCCATCAC-3' and 5'-

TCCACCACCCTGTTGCTGT A-3' for GAPDH. RNA preparation and RT-PCR in the present study were performed in triplicate.

Statistical analysis

The Fisher's PLSD was used to compare the PLLA concentration and relative expression levels of neural specific marker mRNA.
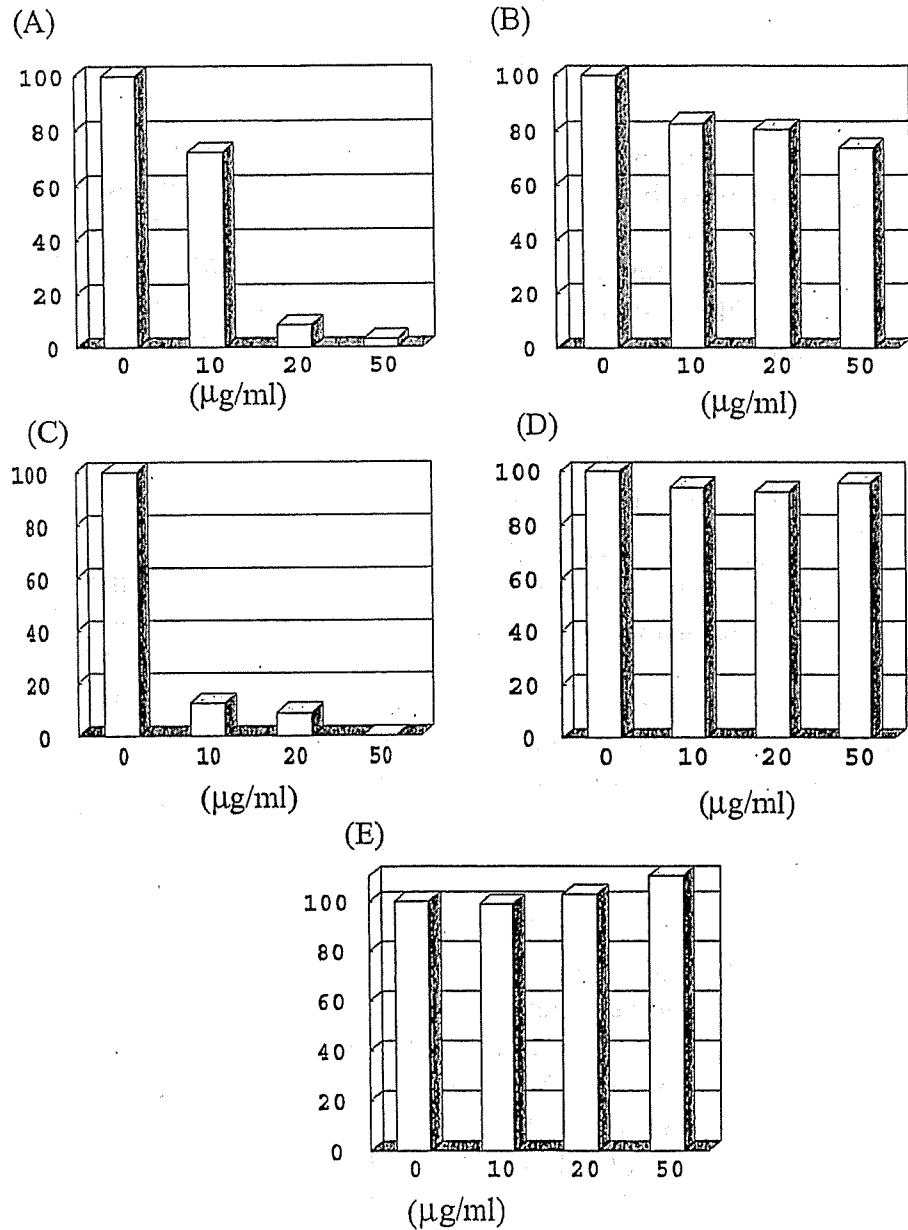

Fig. 1 Effect of PLLA on NHA proliferation (A) PLLA 3.000
(B) PLLA 5.000 (C) PLLA 11.000 (D) Lactic acid (E) Tin chloride

3.   RESULTS AND DISCUSSION

NHA proliferation

We used three kinds of PLLA. PLLA 3000 (PLLA, Mw 3000) is made without catalyst. PLLA 6000 (PLLA, Mw 5000) is made with organic tin catalyst. PLLA 11000 (PLLA, Mw 11000) is made with catalyst tin chloride, contains 590 ppm tin. After a week culture with PLLA, we detected cell number of NHA using MTT assay. Cell numbers were decreased in a dose-dependent manner of PLLA (Fig. 1A-C). The cell number of NHA cultured with 50 µg/ml of PLLA 3000, PLLA 5000 and PLLA 11000 were 15%, 70% and 7.8% of that of control respectively.

Whether tin ion included in PLLA affected NHA proliferation or not, we added tin chloride to NHA culture medium (Fig. 1D). The concentration of tin chloride at 50 ng/ml did not affect NHA proliferation. PLLA is hydrolysed in medium, we assayed lactic acid (LA), a monomer of PLLA was also tested by the MTT assay using NHA cells. (Fig. 1E). There was no effect on the cell number of NHA culture with LA monomer. The cause of PLLA effect for NHA was neither included tin ion nor degraded LA monomer. It was probably the effect of PLLA itself and/or degraded LA oligomers.

Lam and his co-workers demonstrated that predegraded PLLA (P-PLLA; 25 kGy gamma-irradiation) caused signs of cell damage, cell death, and cell lysis due to phagocytosis of a large amount of P-PLLA particles (9). Phagocytosis of LA oligomers or degraded PLLA particles may affect the proliferation and development of NHA. It is necessary to know culture medium with PLLA contains how much PLLA particles, PLLA oligomer and organic tin.

Gene expression of neural cell specific markers

It has been suggested that a part of astrocytes contain neural precursor cell activity that give rise to neuron, oligodendrocyte and astrocyte itself. The recent discovery of stem cell populations in the CNS has generated intense interest, since the brain has long been regarded as incapable of regeneration (5, 10, 11). Neural stem cells (NSCs) have capability for expansion and differentiation into astrocytes, oligodendrocytes, and neurons in vitro (12, 13). NSCs have been suggested to have therapeutic potential for central nervous system regeneration (14-16).

They express their original specific genes, neural cell specific markers. Neural precursor cells express Nestin, a class IV intermediate filament protein. Differentiated neuron expresses Nurr-1, a transcription factor and Id-3, a transcription inhibitory factor. Astrocyte expresses
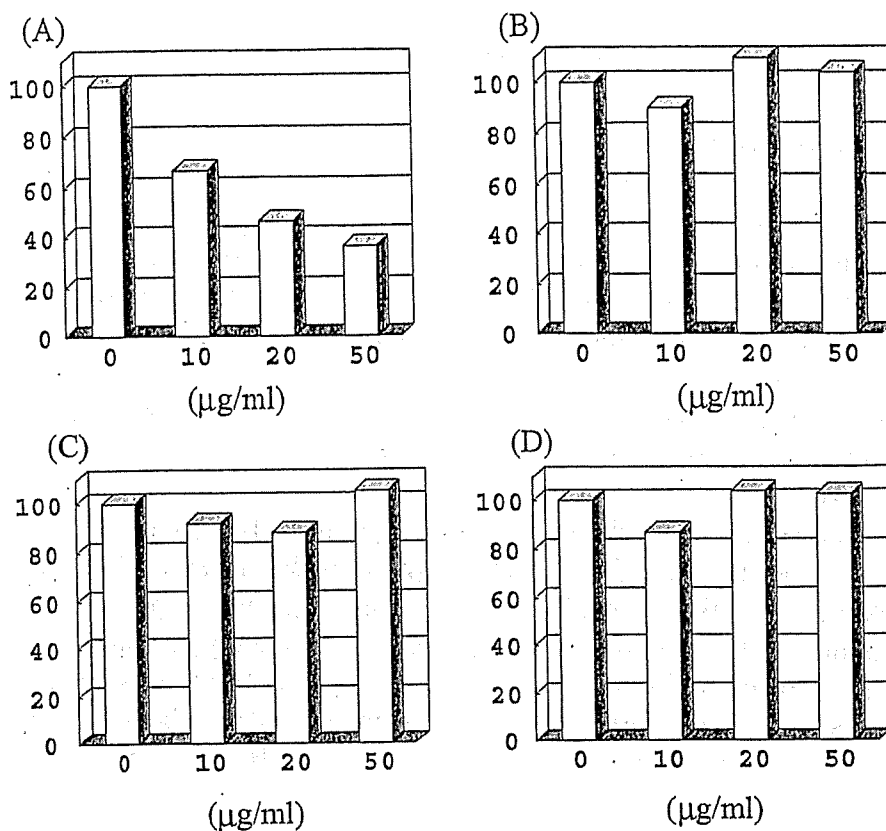
Fig. 2 Effect of PLLA on neural specific gene expression.
(A) Nestin (B) Nurr-1 (C) GFAP (D) Id-3

GFAP, a glial filamentous acidic protein. We compared gene expression of neural cell specific markers. Expression of Nestin, a neural precursor cell marker decreased with the dose of PLLA5000. The expression of Nestin in NHA cultured with 50 µg/ml PLLA was 30% of control (Fig. 2A). Expressions of the other genes that assayed in this study were similar to control (Fig. 2B-D).

Expression of Nestin was decreased when NHA were cultured with PLLA suggested that PLLA decreased population of neural precursor cells. There were two kinds of possibilities. (1) PLLA leads NHA to gliogenesis. Nakashima et al. reported that Gliogenesis significantly reduced the number of cells expressing Nestin and the number of cells expressing microtubule-associated protein 2 (MAP2), a neuronal marker. (2) When neural precursor cells specifically phagocytosed PLLA, they go to programmed cell death, apoptosis or loose their developmental potential as neural precursor cells. Lam et al. demonstrated that PLLA caused signs of cell damage, cell death, and cell lysis due to phagocytosis of a large amount of P-PLLA particles. Phagocytosis of PLLA may affect proliferation and development of NHA.

4.   REFERENCES

[1] McKay, R. (1997) Stem cells in the central nervous system. Science 276, 66-71.

[2] Gage, F. H. (2000) Mammalian neural stem cells. Science 287, 1433-1438.

[3] Nakashima K. et al. (2001) BMP2-mediated alteration in the developmental pathway of fetal mouse brain cells from neurogenesis to astrocytogenesis. Pro. N. A. S. 98, 5868-5873.

[4] Doetsch F. et al. (1999) Subventricular sone astrocytes are neural stem cells in the adult mammalian brain. Cell 97, 703-716.

[5] Johansson C. B. et al. (1999) Identification of a neural stem cell in the adult mammalian central nervous system. Cell 96 25-34.

[6] Gage F. H. et al. (1995) Survival and differentiation of adult neuronal progenitor cells transplantation to the adult brain. Pro. N. A. S. 92, 11879-11883.

[7] Suhonen J. et al. (1996) Differentiation of adult hippocampus-derived progenitors into olfactory neurons in vivo. Nature (London) 383, 624-627.

[8] Tsuchiya T. et al. (2002) Effects of biodegradable polymers on the cellular function of chondrogenesis. (in Japanese) Bio Industry 19, 30-37.

[9] Lam K. H. et al. (1993) The effect of phagcytosis of poly (L-lactic acid) fragments on cellular morphology and viability. J. Biomed. Mater. Res. 27, 1569-1577.

[10] Reynolds B. A. et al. (1992) Generation of neurons and astrocytes from isolated cells of the adult mammalian central nervous system. Science 1707-1710.

[11] Richards L. J. et al. (1992) De novo generation of neuronal cells from the adult mouse brain. Pro. N. A. S. 89, 8591-8595.

[12] Svendsen C. N. et al. (1996) Survival and differentiation of rat and human epidermal growth factor-responsive precursor cells following grafting into the lesioned adult central nervous system. Exp. Neurol. 137, 376-388.

[13] Flax J. D. et al. (1998) Engraftable human neural stem cells respond to development cues, replace neurons, and express foreign genes. Nat. Biotech. 16, 1033-1039.

[14] Woodbury D. et al. (2000) Adult rat and human bone marrow stromal cells differentiate into neurons. J. Neurosci. Res. 61, 364-370.

[15] Sanches-Ramos J. et al. (2000) Adult bone marrow stromal cells differentiate into neural cells in vitro. Exp. Neurol. 164, 247-256.

[16] Deng W. et al. (2001) In vitro differentiation of human marrow stromal cells into early progenitors of neural cells by conditions that increase intracellular cyclic AMP. Biochem. Biophys. Res. Commun. 286, 779-785.

ナノレベルイメージングによる
分子構造と機能の解析

盛　英三　　望月直樹　　武田壮一
井上裕康　　中村　俊　　土屋利江

ナノテクノロジーの臨床　ナノメディシン

ナノレベルイメージングによる分子構造と機能の解析

盛　英三[1]　　望月直樹[1]　　武田壮一[1]
井上裕康[2]　　中村　俊[3]　　土屋利江[4]

Nano-level imaging for analyzing protein structure and function
[1]Hidezo Mori, [1]Naoki Mochizuki, [1]Soichi Takeda,
[2]Hiroyasu Inoue, [3]Shun Nakamura, [4]Toshie Tsuchiya
[1]National Cardiovascular Center Research Institute
[2]Faculty of Human Life and Environment, Nara Women's University
[3]National Center of Neurology and Psychiatry
[4]National Institute of Health Sciences

Abstract

The present manuscript outlines the nano-level imaging project, which is under promotion by the three national research institutes and supported by a research grant from the Ministry of Health, Labor and Welfare (nano-001). This research project targets collecting fundamental information regarding comprehensive understanding of cardiovascular, neurological and the other disorders, developing new diagnostic and therapeutic methods by visualizing protein structure and function in atomic (sub-nano level) or molecular (nano-level) resolution. The results of the current projects will be extended into drug design, clinical diagnostic technology and medical materials in near future.

Key words: nano-technology, structural biology, drug design, protein crystallography, tailor-made medicine

はじめに

21世紀の医療の社会的課題として提唱されているテーラーメード医療の達成には, 標的となる蛋白の構造を患者ごとに確定し(分子診断), 最適な薬剤の構造を選択し(分子治療), 薬剤と生体蛋白の相互作用を分子レベルで観察する(分子評価)などの医療基盤技術の育成が求められる. ナノレベルイメージングプロジェクトでは, 蛋白分子の構造と機能の解析を通じてテーラーメード医療実現のための基盤技術の形成を目指している.

本稿では蛋白構造イメージングを中心に概説する.

1. 創薬に貢献した分子構造イメージング

近年, 放射光を用いたX線回折法の発達により原子レベルの解像度で蛋白結晶の構造を決定できるようになった. 構造に基づく薬剤設計の具体的な成功例として, AIDS治療薬(HIVプロ